Spectral Gap Optimization for Enhanced Adiabatic State Preparation

Kshiti Sneh Rai,[1,2,*] Jin-Fu Chen,[1,2,†] Patrick Emonts,[1,2,3,4,‡] and Jordi Tura[1,2]
[1]Instituut-Lorentz, Universiteit Leiden, P.O. Box 9506, 2300 RA Leiden, The Netherlands
[2]⟨aQa^L⟩ Applied Quantum Algorithms, Universiteit Leiden, The Netherlands
[3]Institute for Complex Quantum Systems, Ulm University, 89069 Ulm, Germany
[4]Center for Integrated Quantum Science and Technology (IQST), Ulm-Stuttgart, Germany

(Received 18 October 2024; revised 5 March 2025; accepted 10 July 2025; published 29 August 2025)

The preparation of nontrivial states is crucial to the study of quantum many-body physics. Such states can be prepared with adiabatic quantum algorithms, which are restricted by the minimum spectral gap along the path. In this Letter, we propose an efficient method to adiabatically prepare tensor network states (TNSs). We maximize the spectral gap leveraging degrees of freedom in the parent Hamiltonian construction. We demonstrate this efficient adiabatic algorithm for preparing TNSs, through examples of random TNSs in one dimension, AKLT (Affleck-Kennedy-Lieb-Tasaki), and GHZ states. The Hamiltonian optimization applies to both injective and non-injective tensors, in the latter case by exploiting symmetries present in the tensors.

DOI: 10.1103/cslt-x32n

Introduction—The preparation of an initial state of interest is the basis for most quantum experiments [1–3]. Given its importance and inherent challenges, quantum many-body state preparation has been approached from various directions [4]. These include gate-based methods [5–11] which are implementable on digital architectures [3,12]. However, the task is not limited to digital devices, as it also constitutes a native operation on analog quantum simulators [13,14].

Adiabatic state preparation involves interpolating a system from the ground state of a trivial Hamiltonian to that of a final Hamiltonian. One key factor influencing the performance of adiabatic algorithms is the minimal spectral gap Δ during the interpolation. Rigorous estimates on the runtime to prepare the ground state of a Hamiltonian yield a scaling $\propto 1/\Delta^3$ [15] and can be improved to $1/\Delta^2$ if certain properties of the gap as a function of the interpolation parameter are known. Developing methods to increase Δ is desirable for designing efficient adiabatic algorithms [8,16,17].

Tensor networks (TNs) comprise a vast family of quantum many-body states that offer additional control over Δ via the so-called parent Hamiltonian (PH) construction. TNs are characterized by an area-law scaling of entanglement across bipartitions [18], and can be expressed concisely with a polynomial number of parameters (in the system size). Moreover, they provide efficient polynomial approximations of ground states of 1D gapped local Hamiltonians [19–21]. Conversely, TNs serve as ground states of a family of local PHs, which can be constructed using the tensor representations [22–26]. An important mathematical property of the tensors is injectivity, which describes the relation between the boundary and bulk of a TN state. If a state has an injective TN representation, then it enables the construction of PHs with *unique* ground states [27], even in arbitrary lattices. Examples of injective matrix product states (MPSs), which are TNs in 1D, include the AKLT state and the cluster state.

The flexibility in the space of PHs allows for the optimization of various quantities. For example in Ref. [28], the proposed algorithm searches for the PH which has an efficient approximation in terms of a Hamiltonian of smaller locality. In this Letter, we actively exploit the nonuniqueness of the PH to optimize the gap during an adiabatic evolution. The algorithm is comprised of the following two steps: (i) We build the parametrized family of PHs with a fixed locality, of a *single* TN state. Following *Weyl's inequality* [29], the spectral gap Δ is a concave function of the free parameters in the PH. The concavity implies that the maximum gap Δ_{opt} and corresponding optimal parameter values of the Hamiltonian can be obtained efficiently using, e.g., a gradient-ascent algorithm. (ii) We fix a deformation of tensors $A(\lambda)$ which interpolates from a product state ($\lambda = 0$) to a state of interest ($\lambda = 1$), ensuring that the intermediate states are also TNs. The TN formulation along the path allows pointwise implementation of the gap optimization, finally

*Contact author: ksrai@lorentz.leidenuniv.nl
†Contact author: jinfuchen@lorentz.leidenuniv.nl
‡Contact author: patrick.emonts@uni-ulm.de

Published by the American Physical Society under the terms of the Creative Commons Attribution 4.0 International license. Further distribution of this work must maintain attribution to the author(s) and the published article's title, journal citation, and DOI.

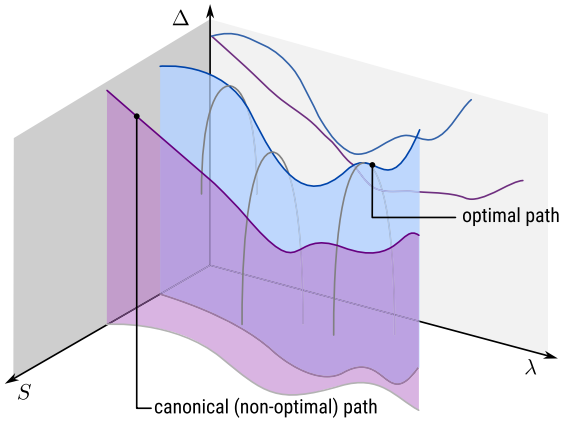


FIG. 1. Sketch of the optimization algorithm. The blue path is the optimized path through the space of Hamiltonians, i.e., it has the maximal gap. The convex optimization in the parameters $\boldsymbol{S}$ is illustrated by gray lines. For comparison, the purple curve is an initial, nonoptimal guess for a path. The actual gap along the path is visualized as a projection on the light-gray Δ-λ plane.

providing a Hamiltonian path $H_{\mathrm{opt}}(\lambda)$ which has a maximum gap at all intermediate points (see Fig. 1).

We illustrate our gap optimization algorithm on exemplary classes of states: the random injective MPS, the AKLT state, and the noninjective GHZ state. In addition, our machinery can effectively incorporate symmetries which allow the method's scalability to larger system sizes and to circumvent the closing of the gap in systems with degenerate ground states. Furthermore, we derive an analytical description of the optimal parameter evolution as a differential equation, which can replace the need for gradient-ascent optimization. The techniques can also be applied when the tensor representation of a TN state is unknown, but one of its PHs is given.

Our Letter contributes to efficient adiabatic preparation methods for TNSs. These are vital in quantum information processing, as they enable protocols for initializing states in quantum phase estimation [5,6,9] and facilitate the study of phenomena such as quantum quenches, dynamics, and the appearance of thermalization in isolated quantum systems [30]. Moreover, the utility of adiabatic methods extends to quantum device verification, as highlighted in Ref. [17].

Preliminaries—Tensor networks constitute a class of states that encode the physical state in a set of tensors which are placed on the vertices of a graph. If two vertices are connected, the associated tensor dimensions are contracted. Concretely, in one spatial dimension, a translation-invariant MPS with periodic boundary conditions can be written as

$$|\psi\rangle = \sum_{\{\sigma\}} \mathrm{Tr}(A^{\sigma_0} A^{\sigma_1} \ldots A^{\sigma_{N-1}}) |\sigma_0 \ldots \sigma_{N-1}\rangle, \tag{1}$$

where A^{σ_i} is a $(D \times D)$ matrix on site $i = 0, \ldots, N-1$ and $\sigma_i = 0, \ldots, d-1$ is the physical index, and D denotes the bond dimension. Given a TNS, we can construct the *local* PHs, i.e., a family of Hamiltonians such that the TNS is the zero energy ground state of each of them. In general, it is trivial to generate a PH for any state by setting $H = \mathbb{1} - |\psi\rangle\langle\psi|$. However, this Hamiltonian is not local by construction. For TNs, the PH $H = \sum_{i=1}^{N} h_i$ of an N-site system can be constructed with the local term

$$h_i = \sum_{\alpha,\beta=1}^{M} S_{\alpha\beta} |\phi_{i,\alpha}\rangle\langle\phi_{i,\beta}| = \Phi_i \boldsymbol{S} \Phi_i^{\dagger}, \tag{2}$$

where $\boldsymbol{S}$ is an arbitrary positive definite matrix normalized to $\mathrm{tr}(\boldsymbol{S}) = 1$, and $\Phi_i = (|\phi_{i,1}\rangle, |\phi_{i,2}\rangle, \ldots, |\phi_{i,M}\rangle)$ is a basis with M elements, obtained using tensors of the state in Eq. (1). For constructing Φ_i, the tensor needs to be *injective* (c.f. [31]), which is achieved by blocking L tensors together, such that $d^L \geq D^2$. While for h_i, the condition changes to strictly larger $d^L > D^2$ for building a L local PH, which is a property required to obtain PHs with the TN as the unique ground state [27]. In the literature, the *canonical* choice of a PH is taken to be $\boldsymbol{S} = \mathbb{1}/M$, where $M = d^L - D^2$. However, the freedom in $\boldsymbol{S}$ can be used to optimize certain properties of the PH, e.g., its locality [28] or its gap. In this Letter we consider the latter (see Fig. 1).

Adiabatic path optimization—Adiabatic algorithms are originally formulated as an interpolation between Hamiltonians as $H = (1-s)H_0 + sH_1$, where $s \in [0,1]$ is the control parameter. In this Letter, we choose a different perspective by deforming the tensors representing the initial and final states. Given an efficient TN representation of the final state, one can express the evolution of the tensor $A := A(\lambda)$ from a $|\psi_{\mathrm{in}}\rangle$ to $|\psi_{\mathrm{fi}}\rangle$, where each tensor entry is a continuous function of a parameter λ, such that $|\psi_{\mathrm{in}}\rangle$ is given by $A(0)$ and $|\psi_{\mathrm{fi}}\rangle$ by $A(1)$. As a result, the state is represented by a TN at all intermediate points, allowing the construction of PHs along the path. Ultimately, this makes it viable to optimize the adiabatic path taken through the Hamiltonian space. We remark, contrary to the usual approaches [38–40], here we do *not* optimize the speed or scheduling of the parameter s. Since the Hamiltonian optimization is distinct from scheduling tasks, it is possible to combine both for improving the overall performance of adiabatic algorithms. Alternatively, there exist gate-based methods [5–7,10,41] to prepare a given TNS directly from the tensors. However, these methods require fine control of the device in terms of gates, which we do not assume in this Letter.

In our technique, the input of the optimization procedure is comprised of the MPS formulation of the state given by tensor $A(\lambda)$ that represents a state, as described in Eq. (1). The concavity of the gap function (c.f. [31]) enables efficient convergence through a gradient descent algorithm along the parameters $\boldsymbol{S}$. First, we obtain the gradient $\partial H/\partial \boldsymbol{S}$ numerically, and then compute the expectation values of

this derivative in the excited state. For small systems, this can be achieved by an exact diagonalization procedure. However, as the size of the system increases, finding low-energy eigenstates and the corresponding spectral gap—becomes computationally intensive [42]. In these cases, we employ excited state density matrix renormalization group (DMRG) to compute both the ground state and the first excited state, therefore the spectral gap [43–45].

The numerical framework presented above suggests the existence of an ideal deformation path, for a given MPS interpolation $\Phi(\lambda)$. We define the *condition of optimality*, which ensures that the gap reaches an extremum at all values of λ during the evolution. Optimality implies that the gradients with respect to the elements of the matrix $\boldsymbol{S}$ are zero at the optimal point,

$$\frac{\partial\Delta(\Phi(\lambda),\boldsymbol{S})}{\partial\boldsymbol{S}}|_{\boldsymbol{S}=\boldsymbol{S}_{\mathrm{opt}}(\lambda)}=0,\qquad\forall\ \lambda\in[0,1],\tag{3}$$

where $\boldsymbol{S}_{\mathrm{opt}}(\lambda)$ denotes the optimal positive definite matrix [c.f. Eq. (2)]. An equivalent formulation of Eq. (3) can be given in terms of the first excited state $|\Psi_1\rangle$ and Φ using χ defined as follows:

$$\chi_{\alpha\beta}\coloneqq\sum_i\langle\Psi_1|\phi_{i,\alpha}\rangle\langle\phi_{i,\beta}|\Psi_1\rangle\tag{4}$$

At the optimal point, under the assumption that χ is full rank, $\boldsymbol{S}_{\mathrm{opt}}$ and χ_{opt} are simultaneously diagonalizable, and additionally, all eigenvalues of χ_{opt} are equal to Δ_{opt}, i.e., $\chi_{\mathrm{opt}}=\Delta_{\mathrm{opt}}\mathbb{1}$, where $\Delta_{\mathrm{opt}}=\Delta(\Phi,\boldsymbol{S}_{\mathrm{opt}})$ is the optimal gap. Generically, $\boldsymbol{S}_{\mathrm{opt}}$ is full rank and the gap is smooth at $\boldsymbol{S}_{\mathrm{opt}}$ although $\boldsymbol{S}_{\mathrm{opt}}(\lambda)$ might not be smooth itself as we will show in examples.

Using the condition of optimality, it is possible to derive an ordinary differential equation (ODE) describing the evolution of $\boldsymbol{S}_{\mathrm{opt}}$ with changing λ. Differentiating Eq. (3) with respect to λ on both sides yields the following ODE:

$$\partial_\lambda\boldsymbol{S}_{\mathrm{opt}}=-(\boldsymbol{H}_{\Delta,\boldsymbol{S}_{\mathrm{opt}}})^{-1}\partial_\Phi\boldsymbol{J}_{\Delta,\boldsymbol{S}_{\mathrm{opt}}}\cdot\partial_\lambda\Phi,\tag{5}$$

where $\boldsymbol{J}_{\Delta,\boldsymbol{S}_{\mathrm{opt}}(\lambda)}=\partial_{\boldsymbol{S}}\Delta|_{\boldsymbol{S}=\boldsymbol{S}_{\mathrm{opt}}(\lambda)}$ and $\boldsymbol{H}_{\Delta,\boldsymbol{S}_{\mathrm{opt}}(\lambda)}=\partial^2_{\boldsymbol{S}}\Delta|_{\boldsymbol{S}=\boldsymbol{S}_{\mathrm{opt}}(\lambda)}$ represent the Jacobian and Hessian of the gap Δ at the optimal $\boldsymbol{S}_{\mathrm{opt}}(\lambda)$ (c.f. [31]), respectively. This formulation leverages optimality [Eq. (3)], bypassing the need for gradient-based optimization and enabling a generalization to higher-dimensional PEPS. Moreover, since it takes the first excited state as input, protocols for eigenstate preparation could benefit from this formulation [46,47].

Random injective MPS preparation—First, we consider the preparation of a random injective MPS using a method proposed by Cruz *et al.* [17]. A matrix product state on a chain of d-dimensional spins is obtained by applying a transformation to a product state of maximally entangled pairs,

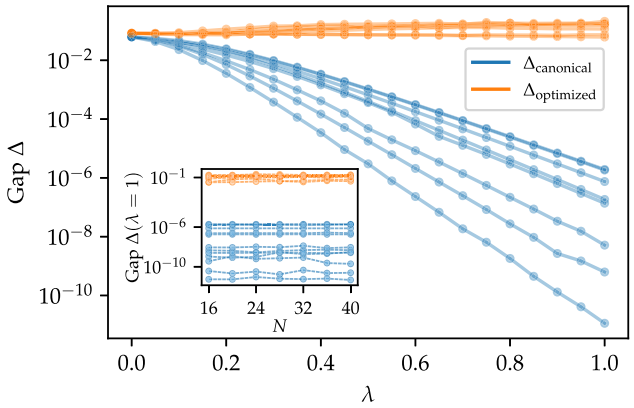


FIG. 2. Gap optimization for the preparation of many random injective MPSs on $N=24$ sites. In all cases, the gap along the path changes from exponentially decaying ($\Delta_{\mathrm{canonical}}$) to roughly constant ($\Delta_{\mathrm{optimized}}$). In the inset, we show the improvement in the gap at $\lambda=1$ for random seeds and system sizes from $N=16$ to $N=40$.

$$|\psi(\mathcal{P})\rangle=\mathcal{P}^{\otimes N}\left(\sum_{i=1}^{d}|ii\rangle\right)^{\otimes N},\tag{6}$$

where $\mathcal{P}$ is defined as a map from the virtual to physical indices. As illustrated in Ref. [17], a smooth path of PHs can be generated by decomposing the map $\mathcal{P}$. With a polar decomposition $\mathcal{P}=QW$, we obtain an isometry W and a positive definite matrix Q. In the case of an injective MPS with $d^L=D^2$, the matrix W is a unitary. By parametrizing $Q=e^{\lambda K_1}$ and $W=e^{iK_2t}$, where K_1 and K_2 are random Hermitian matrices, it is possible to prepare a set of random injective MPSs. In Ref. [17], a canonical form for the PH $H(\lambda,t)$ based on the tensor deformation is proposed which we specialize for translation-invariant MPSs (c.f. [31]).

We start with the product state of spin-1/2 ($d=2$) particles $|\uparrow\rangle^{\otimes N}$ on $N=24$ sites, and generate the map $\mathcal{P}$ using a random choice of (K_1,K_2). These matrices are taken to be the same at all sites, giving the same MPS tensor in the bulk, with bond dimension $D=2$ and physical dimension $d=4$. The value of M [in Eq. (2)] is $M=d^2-D^2=4^2-2^2=12$. Figure 2 compares the spectral gap of canonical Hamiltonian $H(\lambda,t)$ in comparison with the optimized Hamiltonian $H_{\mathrm{opt}}(\lambda,t)$, with the constructions explained in detail in Sec. IV of Ref. [31]. $\Delta_{\mathrm{canonical}}(\lambda,t)$ is found to decay exponentially with λ, while after the optimization, the gaps of $\Delta_{\mathrm{optimized}}(\lambda,t)$ are approximately constant during the evolution. In the inset, we show that the difference between the optimized and unoptimized gaps of the PH of the final MPS remains exponentially large with increasing system size N.

Adiabatic preparation of the AKLT state—Next, we optimize the preparation of the 1D AKLT state [48] starting from a trivial product modified of spin-1 ($d=3$) particles. In contrast to random MPS states, this state has

considerably more symmetries which we will include later. We interpolate the MPS tensors along a linear path,

$$A^{(-1)} = \begin{pmatrix} 0 & 0 \\ \lambda & 0 \end{pmatrix}, \qquad A^{(0)} = \frac{1}{\sqrt{2}} \begin{pmatrix} 1 & 0 \\ 0 & -\lambda \end{pmatrix},$$
$$A^{(+1)} = \begin{pmatrix} 0 & -\lambda \\ 0 & 0 \end{pmatrix}. \tag{7}$$

This MPS becomes injective upon blocking two sites, and the dimension M [in Eq. (2)] is $M = d^2 - D^2 = 5$. The basis states $\{|\phi_{i,\alpha}(\lambda)\rangle\}_{\alpha=1}^{5}$ for the kernel are parameterized such that at $\lambda = 1$ they represent the Dicke states of the spin-2 subspace. In many physical cases, the spectral gap can be enhanced additionally by exploiting the symmetry of the MPS tensors. The symmetries [49] in the AKLT state include (i) translation invariance, since it is a periodic MPS, (ii) conservation of total S^z: $\langle S^z_{\text{tot}} \rangle = 0$, which appears due to the valence bond structure of the state, and (iii) a type of $\mathbb{Z}_2$ symmetry: with $Q = \prod_{i=1}^{N} F_i \mathcal{I}$, where the operation $\mathcal{I}$ is the inversion operator and F_i is the flip operator [50] on site i, that maps $|+1\rangle \overset{F}{\leftrightarrow} |-1\rangle$, and preserves the $|0\rangle$ state. Upon including these symmetries (c.f. [31]), the positive matrix $\boldsymbol{S}$ simplifies to

$$\boldsymbol{S} = \text{diag}(S_{11}, S_{22}, 1 - 2S_{11} - 2S_{22}, S_{22}, S_{11}). \tag{8}$$

Thus, the number of parameters is reduced from 5 to 2. This form for $\boldsymbol{S}$ corresponds to a basis choice for the spin-2 subspace arising from the addition of angular momentum of two spin-1 particles. As a reference for the optimization, we take the standard canonical choice, $\boldsymbol{S} = \mathbb{1}/5$. After applying the gradient-ascent optimization on $N = 30$ sites, we see an improvement in the gap [Fig. 3(a)]. The SU(2) symmetry is only present at $\lambda = 1$, corresponding to the AKLT state [51]. Hence, the optimal PH remains different from the canonical ones. When the family of PHs is expressed in the symmetric basis of the MPS, the original energy spectrum splits into parts—each with a different value of the quantum number of the symmetry under consideration. In the block-diagonalized form of the Hamiltonian, this means that the allowed states lie only within a specific block, excluding other sectors. We depict this for the AKLT state in Fig. 3(b). In the subspace containing the ground state, there can be two improvements: (i) the spectral gap is larger, since the new first excited state can be one of the higher energy eigenstates of the original Hamiltonian, (ii) a noninjective state becomes a unique ground state, which is demonstrated in the next example of a GHZ state.

Adiabatic preparation of the GHZ state—Up to now, we have focused on the case of injective MPSs, which are unique ground states of PHs constructed using Eq. (2). The same construction in the case of noninjective MPSs, leads to a Hamiltonian with a degenerate ground space.

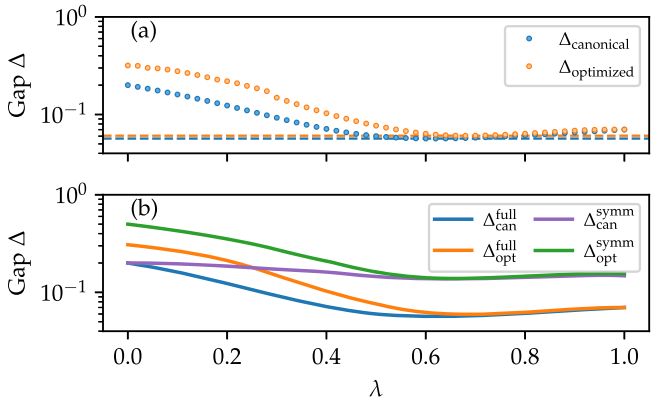


FIG. 3. Preparation of the AKLT state using MPS tensors defined in Eq. (7). (a) The blue and orange points show spectral gaps along the adiabatic path for canonical and optimized Hamiltonians, respectively for $N = 30$ and periodic boundary conditions. The horizontal dashed lines indicate the minimum gap along each path. (b) Comparison of the spectral gaps of canonical and optimized Hamiltonians with those in the symmetry sector containing the ground state on a system of $N = 8$ sites. The labels "full" and "symm" refer to the full Hilbert space and the symmetric subspace associated with the ground state, respectively. Δ_{can} and Δ_{opt} denote the canonical and optimized gaps.

The degeneracy can hinder the adiabatic preparation, either when targeting a noninjective MPS as the final state or encountering it as an intermediate state before reaching an injective MPS. In these situations, it is possible to avoid degeneracies by restricting to a symmetric subspace. To demonstrate this, we choose the spin-$\frac{1}{2}$ ($d = 2$) GHZ state which appears during adiabatic evolution between the (ordered) product state MPS ($\lambda = -1$), where all spins align in the x direction; and (disordered) cluster state ($\lambda = 1$) [52] of spin-$\frac{1}{2}$ particles, given by the following tensors:

$$A_0 = \begin{pmatrix} 0 & 0 \\ 1 & 1 \end{pmatrix}, \qquad A_1 = \begin{pmatrix} 1 & -\lambda \\ 0 & 0 \end{pmatrix}. \tag{9}$$

The locality of the PH for the above tensor is $L = 3$ and $M = d^3 - D^2 = 4$. At $\lambda = 0$, the above tensor corresponds to the GHZ state, which is noninjective, and the family of PHs generated by Eq. (2) becomes twofold degenerate. Thus, in the full Hilbert space, the spectral gap closes as λ approaches 0 [c.f. orange curve in panel (a) of Fig. 4]. To lift this degeneracy, we impose conservation of parity of the σ_x operator $P = \prod_{i=1}^{N} \sigma_i^x$, to be $+1$, enforcing a nonzero gap (c.f. purple curve in Fig. 4). However, the gap still decays with increasing system size and at sufficiently large N, the optimized gaps converge to the gaps of the canonical Hamiltonian ($\boldsymbol{S} = \mathbb{1}/4$) [c.f. Fig. 4(b)]. For comparison, we have plotted the analytical form for the gap in the

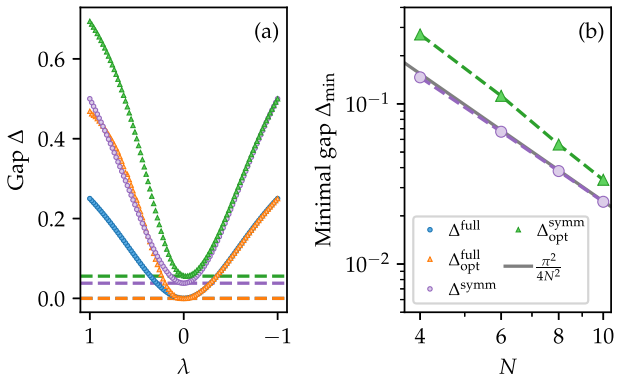


FIG. 4. (a) Illustration of gaps along the canonical (can) and optimized (opt) adiabatic path for $N = 8$ sites sweeping from the product state ($\lambda = -1$) to cluster state ($\lambda = 1$), crossing the GHZ state at ($\lambda = 0$); full refers to the full Hilbert space, symm to the symmetric subspace with the ground state. (b) Minimum gaps in the symmetric subspace along the path plotted in log-log scale. The solid line corresponds to analytically formula for the gap in the symmetric subspace. The orange and blue lines are not plotted in the right plot, as they remain zero ($\sim 10^{-15}$) for all N.

symmetric subspace, given as $\Delta_N \approx \pi^2/(4N^2)$ for the case of $(\boldsymbol{S} = \mathbb{1}/4)$.

Conclusion and outlook—In this Letter, we optimize the Hamiltonian path for preparing specific TNSs adiabatically. We interpolate between the MPS tensors and build the corresponding PHs with a maximum gap along the path. We rely on geometric locality since the PH construction of tensor network states requires the support to be on neighboring sites. This is an appealing feature for experimental setups, as geometric locality is the desired form of interaction [1,53–57]. We demonstrate our algorithm in three paradigmatic cases, yielding uniformly better gaps in all. Finally, we formulate a differential equation for the optimal parameters, yielding an implicit solution equivalent to pointwise optimization.

The optimization method can generally accelerate the adiabatic preparation of all short-range correlated states, where the gap during the path admits a nontrivial constant lower bound. This also allows for preparing topological states with nontrivial SPT order, as demonstrated for the AKLT state. Notably, both the interpolated state for arbitrary λ in Eq. (7) and the corresponding PHs [Eq. (2)], break the symmetry defining the SPT order (as numerically shown in Sec. V(B) of [31]), resulting in a nonclosing gap in our PH construction.

Our research opens up several future questions. Our technique requires the spectral gap of the PH, which may be hard to obtain. A natural next step is to use alternative methods for gap estimation. These are based on semidefinite programming [17,58,59] and extend beyond the validity of DMRG, e.g., allowing a generalization to higher-dimensional geometries and the thermodynamic limit. Additionally, the fidelity of the final state depends not only on the gap, but also on the speed of traversal [38,40]. The combined optimization of speed and spectral gap is expected to further enhance the efficiency of adiabatic preparation algorithms.

Acknowledgments—We thank Norbert Schuch, Esther Cruz Rico, Benjamin Schiffer, Stefano Polla, Georgios Styliaris, Ilya Kull, Flavio Baccari, Zhi-Yuan Wei, and Anastasiia Skurativska for useful discussions. P. E. and J. T. acknowledge the support received by the Dutch National Growth Fund (NGF), as part of the Quantum Delta NL programme. P. E. acknowledges the support received through the NWO-Quantum Technology programme (Grant No. NGF.1623.23.006). P. E. further acknowledges funding by the Carl-Zeiss-Stiftung (CZS Center QPhoton). K. S. R., J. F. C., and J. T. acknowledge the support received from the European Union's Horizon Europe research and innovation programme through the ERC StG FINE-TEA-SQUAD (Grant No. 101040729). This publication is part of the "Quantum Inspire—the Dutch Quantum Computer in the Cloud" project (with Project No. [NWA.1292.19.194]) of the NWA research program "Research on Routes by Consortia (ORC)," which is funded by the Netherlands Organization for Scientific Research (NWO). Parts of this work were performed by using the computing resources from the Academic Leiden Interdisciplinary Cluster Environment (ALICE) provided by Leiden University.

The views and opinions expressed here are solely those of the authors and do not necessarily reflect those of the funding institutions. Neither of the funding institutions can be held responsible for them.

Data availability—The code [60] used and the data [61] that support the findings of this article are openly available.

[1] H. Bernien, S. Schwartz, A. Keesling, H. Levine, A. Omran, H. Pichler, S. Choi, A. S. Zibrov, M. Endres, M. Greiner, V. Vuletić, and M. D. Lukin, Probing many-body dynamics on a 51-atom quantum simulator, Nature (London) **551**, 579 (2017).

[2] S. Ebadi, T. T. Wang, H. Levine, A. Keesling, G. Semeghini, A. Omran, D. Bluvstein, R. Samajdar, H. Pichler, W. W. Ho, S. Choi, S. Sachdev, M. Greiner, V. Vuletić, and M. D. Lukin, Quantum phases of matter on a 256-atom programmable quantum simulator, Nature (London) **595**, 227 (2021).

[3] R. Barends *et al.*, Digitized adiabatic quantum computing with a superconducting circuit, Nature (London) **534**, 222 (2016).

[4] A. Montanaro, Quantum algorithms: An overview, npj Quantum Inf. **2**, 15023 (2016).

[5] C. Schön, E. Solano, F. Verstraete, J. I. Cirac, and M. M. Wolf, Sequential generation of entangled multiqubit states, Phys. Rev. Lett. **95**, 110503 (2005).

[6] S.-J. Ran, Encoding of matrix product states into quantum circuits of one- and two-qubit gates, Phys. Rev. A **101**, 032310 (2020).
[7] K. C. Smith, E. Crane, N. Wiebe, and S. Girvin, Deterministic constant-depth preparation of the AKLT state on a quantum processor using fusion measurements, PRX Quantum **4**, 020315 (2023).
[8] Z.-Y. Wei, D. Malz, and J. I. Cirac, Efficient adiabatic preparation of tensor network states, Phys. Rev. Res. **5**, L022037 (2023).
[9] S. Fomichev, K. Hejazi, M. S. Zini, M. Kiser, J. F. Morales, P. A. M. Casares, A. Delgado, J. Huh, A.-C. Voigt, J. E. Mueller, and J. M. Arrazola, Initial state preparation for quantum chemistry on quantum computers, PRX Quantum **5**, 040339 (2024).
[10] D. Malz, G. Styliaris, Z.-Y. Wei, and J. I. Cirac, Preparation of matrix product states with log-depth quantum circuits, Phys. Rev. Lett. **132**, 040404 (2024).
[11] C. Mc Keever and M. Lubasch, Towards adiabatic quantum computing using compressed quantum circuits, PRX Quantum **5**, 020362 (2024).
[12] G. Wendin, Quantum information processing with superconducting circuits: A review, Rep. Prog. Phys. **80**, 106001 (2017).
[13] J. I. Cirac and P. Zoller, Goals and opportunities in quantum simulation, Nat. Phys. **8**, 264 (2012).
[14] C. Gross and I. Bloch, Quantum simulations with ultracold atoms in optical lattices, Science **357**, 995 (2017).
[15] S. Jansen, M.-B. Ruskai, and R. Seiler, Bounds for the adiabatic approximation with applications to quantum computation, J. Math. Phys. (N.Y.) **48**, 102111 (2007).
[16] Y. Ge, A. Molnár, and J. I. Cirac, Rapid adiabatic preparation of injective projected entangled pair states and Gibbs states, Phys. Rev. Lett. **116**, 080503 (2016).
[17] E. Cruz, F. Baccari, J. Tura, N. Schuch, and J. I. Cirac, Preparation and verification of tensor network states, Phys. Rev. Res. **4**, 023161 (2022).
[18] F. Verstraete and J. I. Cirac, Matrix product states represent ground states faithfully, Phys. Rev. B **73**, 094423 (2006).
[19] I. Cirac, D. Perez-Garcia, N. Schuch, and F. Verstraete, Matrix product states and projected entangled pair states: Concepts, symmetries, and theorems, Rev. Mod. Phys. **93**, 045003 (2021).
[20] M. B. Hastings and T. Koma, Spectral gap and exponential decay of correlations, Commun. Math. Phys. **265**, 781 (2006).
[21] M. B. Hastings, An area law for one-dimensional quantum systems, J. Stat. Mech. (2007) P08024.
[22] M. Fannes, B. Nachtergaele, and R. F. Werner, Finitely correlated states on quantum spin chains, Commun. Math. Phys. **144**, 443 (1992).
[23] D. Perez-Garcia, F. Verstraete, M. M. Wolf, and J. I. Cirac, Matrix product state representations, Quantum Inf. Comput. **7**, 401 (2007).
[24] N. Schuch, I. Cirac, and D. Pérez-García, PEPS as ground states: Degeneracy and topology, Ann. Phys. (Amsterdam) **325**, 2153 (2010).
[25] N. Schuch, D. Perez-Garcia, and I. Cirac, Classifying quantum phases using matrix product states and PEPS, Phys. Rev. B **84**, 165139 (2011).
[26] N. Schuch, A. Molnar, and D. Perez-Garcia, Simple Hamiltonians for matrix product state models, arXiv:2503.10767.
[27] D. Perez-Garcia, F. Verstraete, J. I. Cirac, and M. M. Wolf, PEPS as unique ground states of local Hamiltonians, Quantum Inf. Comput. **8**, 0650 (2008).
[28] G. Giudici, J. I. Cirac, and N. Schuch, Locality optimization for parent Hamiltonians of tensor networks, Phys. Rev. B **106**, 035109 (2022).
[29] H. Weyl, Das asymptotische Verteilungsgesetz der Eigenwerte linearer partieller Differentialgleichungen (mit einer Anwendung auf die Theorie der Hohlraumstrahlung), Math. Ann. **71**, 441 (1912).
[30] A. Polkovnikov, K. Sengupta, A. Silva, and M. Vengalattore, Colloquium: Nonequilibrium dynamics of closed interacting quantum systems, Rev. Mod. Phys. **83**, 863 (2011).
[31] See Supplemental Material at http://link.aps.org/supplemental/10.1103/cslt-x32n for numerical details and background on the parent Hamiltonian derivation, which includes Refs. [32–37].
[32] P. Güttinger, Das Verhalten von Atomen im magnetischen Drehfeld, Z. Phys. **73**, 169 (1932).
[33] J. Hauschild and F. Pollmann, Efficient numerical simulations with Tensor Networks: Tensor Network PYTHON (TeNPy), SciPost Physics Lecture Notes, 5 (2018).
[34] J. Gray, Quimb: A PYTHON package for quantum information and many-body calculations, J. Open Source Software **3**, 819 (2018).
[35] X. Chen and A. Vishwanath, Towards Gauging time-reversal symmetry: A tensor network approach, Phys. Rev. X **5**, 041034 (2015).
[36] F. Pollmann, A. M. Turner, E. Berg, and M. Oshikawa, Entanglement spectrum of a topological phase in one dimension, Phys. Rev. B **81**, 064439 (2010).
[37] R. Fletcher, *Practical Methods of Optimization*, 1st ed. (Wiley, New York, 2000).
[38] B. F. Schiffer, J. Tura, and J. I. Cirac, Adiabatic spectroscopy and a variational quantum adiabatic algorithm, PRX Quantum **3**, 020347 (2022).
[39] A. Negretti, A. Benseny, J. Mompart, and T. Calarco, Speeding up the spatial adiabatic passage of matter waves in optical microtraps by optimal control, Quantum Inf. Process. **12**, 1439 (2013).
[40] J.-F. Chen, Speeding up quantum adiabatic processes with dynamical quantum geometric tensor, Phys. Rev. Res. **4**, 023252 (2022).
[41] Z.-Y. Wei, D. Malz, and J. I. Cirac, Sequential generation of projected entangled-pair states, Phys. Rev. Lett. **128**, 010607 (2022).
[42] T. Cubitt, D. Perez-Garcia, and M. M. Wolf, Undecidability of the spectral gap (short version), Nature (London) **528**, 207 (2015).
[43] S. R. White, Density matrix formulation for quantum renormalization groups, Phys. Rev. Lett. **69**, 2863 (1992).
[44] U. Schollwöck, The density-matrix renormalization group in the age of matrix product states, Ann. Phys. (Amsterdam) **326**, 96 (2011).

[45] E. M. Stoudenmire and S. R. White, Studying two dimensional systems with the density matrix renormalization group, Annu. Rev. Condens. Matter Phys. **3**, 111 (2012).
[46] R. Santagati, J. Wang, A. A. Gentile, S. Paesani, N. Wiebe, J. R. McClean, S. Morley-Short, P. J. Shadbolt, D. Bonneau, J. W. Silverstone, D. P. Tew, X. Zhou, J. L. O'Brien, and M. G. Thompson, Witnessing eigenstates for quantum simulation of Hamiltonian spectra, Sci. Adv. **4**, eaap9646 (2018).
[47] J. Tilly, H. Chen, S. Cao, D. Picozzi, K. Setia, Y. Li, E. Grant, L. Wossnig, I. Rungger, G. H. Booth, and J. Tennyson, The variational quantum eigensolver: A review of methods and best practices, Phys. Rep. **986**, 1 (2022).
[48] I. Affleck, T. Kennedy, E. H. Lieb, and H. Tasaki, Rigorous results on valence-bond ground states in antiferromagnets, Phys. Rev. Lett. **59**, 799 (1987).
[49] S. Moudgalya, S. Rachel, B. A. Bernevig, and N. Regnault, Exact excited states of nonintegrable models, Phys. Rev. B **98**, 235155 (2018).
[50] The matrix for the flip operator is, $F = \begin{pmatrix} 0 & 0 & 1 \\ 0 & 1 & 0 \\ 1 & 0 & 0 \end{pmatrix}$.
[51] I. Affleck, Quantum spin chains and the Haldane gap, J. Phys. Condens. Matter **1**, 3047 (1989).
[52] M. M. Wolf, G. Ortiz, F. Verstraete, and J. I. Cirac, Quantum phase transitions in matrix product systems, Phys. Rev. Lett. **97**, 110403 (2006).
[53] J. I. Cirac and P. Zoller, Quantum computations with cold trapped ions, Phys. Rev. Lett. **74**, 4091 (1995).
[54] A. Sørensen and K. Mølmer, Quantum computation with ions in thermal motion, Phys. Rev. Lett. **82**, 1971 (1999).
[55] T. C. Ralph, K. J. Resch, and A. Gilchrist, Efficient Toffoli gates using qudits, Phys. Rev. A **75**, 022313 (2007).
[56] H. Weimer, M. Müller, I. Lesanovsky, P. Zoller, and H. P. Büchler, A Rydberg quantum simulator, Nat. Phys. **6**, 382 (2010).
[57] L. Isenhower, M. Saffman, and K. Mølmer, Multibit C k NOT quantum gates via Rydberg blockade, Quantum Inf. Process. **10**, 755 (2011).
[58] I. Kull, N. Schuch, B. Dive, and M. Navascués, Lower bounding ground-state energies of local Hamiltonians through the renormalization group, Phys. Rev. X **14**, 021008 (2024).
[59] K. S. Rai, I. Kull, P. Emonts, J. Tura, N. Schuch, and F. Baccari, A Hierarchy of Spectral Gap Certificates for Frustration-Free Spin Systems, arXiv:2411.03680.
[60] Code: https://gitlab.com/patrick.emonts/gap-optimization
[61] Data: https://gitlab.com/patrick.emonts/gap-optimization-data